General Disclaimer

One or more of the Following Statements may affect this Document

- This document has been reproduced from the best copy furnished by the organizational source. It is being released in the interest of making available as much information as possible.

- This document may contain data, which exceeds the sheet parameters. It was furnished in this condition by the organizational source and is the best copy available.

- This document may contain tone-on-tone or color graphs, charts and/or pictures, which have been reproduced in black and white.

- This document is paginated as submitted by the original source.

- Portions of this document are not fully legible due to the historical nature of some of the material. However, it is the best reproduction available from the original submission.

Produced by the NASA Center for Aerospace Information (CASI)

X-643-69-391

PREPRINT

NASA TM X- 63675

A DESCRIPTION OF POSITION ANGLES FROM THE HODOGRAPH OF A CENTRAL FIELD MOTION

J. B. EADES, JR.

OCT 1969
RECEIVED
NASA STI FACILITY
INPUT BRANCH

SEPTEMBER 1969

GSFC

GODDARD SPACE FLIGHT CENTER
GREENBELT, MARYLAND

N69-37615
(ACCESSION NUMBER) (THRU)
41 1
(PAGES) (CODE)
NASA-TMX-#63675 30
(NASA CR OR TMX OR AD NUMBER) (CATEGORY)
FACILITY FORM 602

X-643-69-391
Preprint

A DESCRIPTION OF POSITION ANGLES FROM THE HODOGRAPH OF A CENTRAL FIELD MOTION

J. B. Eades, Jr.*

September, 1969

*NRC-NASA Resident Research Associate, on leave from Virginia Polytechnic Institute, Blacksburg, Virginia.

Goddard Space Flight Center
Greenbelt, Maryland

PRECEDING PAGE BLANK NOT FILMED.

CONTENTS

PRECEDING PAGE BLANK NOT FILMED.

A DESCRIPTION OF POSITION ANGLES FROM THE HODOGRAPH OF A CENTRAL FIELD MOTION

ABSTRACT

The velocity hodograph, representing a two-body motion, can be used in the development of analytic relations which are descriptive of this category of central field trajectories. In this paper a brief vector development is presented which leads directly to the two principal velocity hodograph representations; namely, the "classical" hodograph and the "special" hodograph. As an example of the utility of these representations a geometric description of, and correlation between, the several position angles of reference (true, eccentric and mean anomalies) is developed, as appropriate.

NOTATION

$\mathcal{A}$, $\mathcal{P}$	describing apocenter and pericenter locations, respectively.
a	semimajor axis length
$\mathcal{C}$, R	parameters associated with the hodograph (See equation (8))
$\bar{e}_i$	unit vector ($i = r, \varphi, z; x, y, z$).
E	specific energy for a body in motion ($E = (V^2/2) - (\mu/r)$).
$\mathcal{E}$	eccentric anomaly
$\mathcal{E}_H$	hyperbolic analog to the eccentric anomaly.
F, F*	occupied, unoccupied foci.
h	specific angular momentum
H	an angle of reference for a hyperbolic trajectory
M	mean anomaly
M_H	the analog for mean anomaly referred to a hyperbolic trajectory
n	mean motion, elliptic path
n_H	mean motion, hyperbolic path
P	a general position on a trajectory
p	focal parameter ($p \triangleq h^2/\mu = a\,\lvert 1 - \epsilon^2 \rvert$)
Q, J, D, O	position indicators in the constructions described herein

r radius to a trajectory position, measured from F

r, φ, z polar coordinates, associated with the moving triad $(\bar{e}_r, \bar{e}_\varphi, \bar{e}_z)$

t time

$\bar{V}, V_i$ Velocity vector, and speed components ($i = r, \varphi, x, y$)

$V(\varphi), V(y)$ speed components defined on Figure 2

x, y, z cartesian coordinates, associated with the trajectory-fixed triad $(\bar{e}_x, \bar{e}_y, \bar{e}_z)$

β, γ elevation angles referred to the V_x, V_y and V_r, V_φ speed components, respectively.

$\epsilon, \bar{\epsilon}$ eccentricity (scalar, vector)

μ gravitational constant

τ time of pericenter passage.

Subscripts, Superscripts

$(\ )_{lim}$ a limit value

$(\dot{\ }), (\ddot{\ })$ orders of differentiation, with respect to time.

A DESCRIPTION OF POSITION ANGLES FROM THE HODOGRAPH OF A CENTRAL FIELD MOTION

INTRODUCTION

In recent years there has been a renewed interest in hodograph methods, particularly where these apply to orbital mechanics and space flight operations. The works of several authors (1-4)* have contributed materially to this growth of this method; and have been instrumental in developing useful analytic and geometric tools for application purposes.

The hodograph method is generally thought of as a novel technique used as a check on analytic methods; however, the geometry itself can be used to describe orbital motions and to link orbital parameters, as well as serving in the development of a variety of analytical expressions. Even though the hodograph presents a space trajectory as an abstract geometry it can very readily augment and simplify the physical system once an investigator has become familiar with its meaning and interpretation. Quite frequently the hodograph will provide a simplification to aid in the understanding of some particular problem at hand. At other times it affords a direct means for representing rather complicated mathematical expressions in a simple and unique graphical manner.

*Refers to references noted at the end of this paper.

In this paper the hodograph of a two-body motion will be used to describe (geometrically) the eccentric anomaly and mean anomaly, as these quantities relate to the position angle (or, true anomaly) for a space trajectory. In this regard the investigation will be concerned with the two primary trajectory types—the elliptic and the hyperbolic.

Basic Development

In this analysis a simple two-body, central field problem is assumed. The motion will be described in reference to two basic coordinate frames of reference—one which moves, following the motion about the trajectory; and, one which is fixed relative to the flight path proper. Let the moving frame be described by a moving unit triad $(\bar{e}_r, \bar{e}_\varphi, \bar{e}_z)$, while the fixed frame will be related to the fixed unit triad $(\bar{e}_x, \bar{e}_y, \bar{e}_z)$; see Figure 1.

In this section the basic developments will be undertaken. These will lead to a particular description of the velocity vector for the motion. Subsequently, this expression will be utilized to define the hodograph(s) and to obtain other information pertinent to the motion along the flight path.

For a description of the two-body trajectory, and that of the velocity vector, one may begin with the specific equation of motion

$$\ddot{\bar{r}} = - \frac{\mu}{r^2} \bar{e}_r \tag{1}$$

where μ is the appropriate gravitational constant and $\bar{r}$ is the position vector; $\bar{r} \triangleq r\bar{e}_r$! If equation (1) is vectorally multiplied by $\bar{r}$, then

$$\bar{r} \times \ddot{\bar{r}} = -\frac{\mu}{r^2}(\bar{r} \times \bar{e}_r) \equiv 0 \qquad (2)$$

since $\bar{r}$ and $\bar{e}_r$ are parallel vectors. Recognizing that

$$\bar{r} \times \ddot{\bar{r}} \equiv \frac{d}{dt}(\bar{r} \times \dot{\bar{r}}), \qquad (3)$$

then Equation (2) suggests

$$\bar{r} \times \dot{\bar{r}} \overset{\Delta}{=} \bar{h} \text{ (constant)}, \qquad (3)$$

which is the familiar expression for the (fixed) specific moment of momentum.

Next, let equation (1) be multiplied (vectorially) by $\bar{h}$; that is,

$$\bar{h} \times \ddot{\bar{r}} = -\frac{\mu}{r^2}(\bar{h} \times \bar{e}_r) \equiv -\mu \frac{d}{dt}(\bar{e}_r) \qquad (4)$$

wherein, $\bar{e}_r \overset{\Delta}{=} \bar{r}/r$. However, since $\bar{h}$ and μ are constants, then a first integral from equation (4) would give

$$\dot{\bar{r}} \times \bar{h} = \mu(\bar{e}_r + \bar{\epsilon}), \qquad (5)$$

wherein $\bar{\epsilon}$ plays the role of an integration constant.

When equation (5) is scalar multiplied by $\bar{r}$, one obtains

$$r = \frac{h^2/\mu}{1 + \bar{e}_r \cdot \bar{\epsilon}} \qquad (6a)$$

which, when compared to the more familiar form of the conic equation

$$r = \frac{p}{1 + \epsilon \cos \varphi}, \tag{6b}$$

leads to the conclusions that: (1) p (the focal parameter) $\overset{\Delta}{=} h^2/\mu$; and, (2) $\bar{\epsilon}$ is the eccentricity vector. Assuming that $\varphi = 0$ corresponds to periapsis then $\bar{\epsilon} \overset{\Delta}{=} \epsilon\, \bar{e}_x$; and $\bar{e}_r \cdot \bar{\epsilon} \equiv \epsilon \cos\varphi$, which indicates that $|\bar{\epsilon}| = \epsilon$, and $\bar{e}_r \cdot \bar{e}_x = \cos \varphi$ (see Figure 1).

A Unique Description of the Velocity Vector

To describe the velocity vector for this motion, equation (5) is multiplied (vectorially) by $\bar{h}$; thus

$$\bar{h} \times (\dot{\bar{r}} \times \bar{h}) = \mu\, [\bar{h} \times (\bar{e}_r + \bar{\epsilon})]. \tag{7}$$

Since, from equation (3) $\bar{h} = h\bar{e}_z$, then it follows that the triple vector product on the left of equation (7) can be replaced as noted below:

$$\bar{h} \times (\dot{\bar{r}} \times \bar{h}) = \dot{\bar{r}}(\bar{h} \cdot \bar{h}) - \bar{h}(\bar{h} \cdot \dot{\bar{r}}) \equiv \dot{\bar{r}}(\bar{h} \cdot \bar{h}),$$

since $\bar{h} \cdot \dot{\bar{r}} = 0$! The vector multiplication of the right of equation (7) can be carried out directly; this leads to the following description of the velocity vector,

$$\bar{V} = \frac{\mu}{h} (\bar{e}_\varphi + \epsilon\, \bar{e}_y), \tag{8}$$

which will be symbolically written as $\bar{V} = \not{C}\,\bar{e}_\varphi + R\,\bar{e}_y$.

This expression, equation (8), is somewhat unusual in that the two component vectors, in the $\bar{e}_\varphi$ and $\bar{e}_y$ directions, have fixed magnitudes and are not generally orthogonal components. In fact the complete velocity vector is composed of: (1) a vector of fixed magnitude following the motion about the conic; and (2) , a fixed vector relative to the orbit proper. (To aid in understanding this description, Figure 2 has been included). Note that the vector $\bar{V}(\varphi) \overset{\Delta}{=} (\mu/h)\bar{e}_\varphi$ changes direction as one moves about the orbit, while the vector $\bar{V}(y) \overset{\Delta}{=} \epsilon(\mu/h)\bar{e}_y$ is fixed in direction and magnitude for all points on the trajectory. Even though Figure 2 represents an ellipse, equation (8) is general and refers to any free, two body, central field conic.

The Velocity Components

To obtain the speed components in a given direction, parallel to the various coordinate axes, one forms the appropriate scalar products, using equation (8); that is, $\bar{V}_i \overset{\Delta}{=} \bar{V} \cdot \bar{e}_i$ $(i = r, \varphi;\ x, y)$.

or

$$V_\varphi = \not{C}\,(\bar{e}_\varphi + \epsilon\,\bar{e}_y) \cdot \bar{e}_\varphi = \not{C}\,(1 + \epsilon \cos\varphi),$$

$$V_r = \not{C}\,(\bar{e}_\varphi + \epsilon\,\bar{e}_y) \cdot \bar{e}_r = \not{C}\,\epsilon \sin\varphi\,;$$

and (9)

$$V_x = \not{C}\,(\bar{e}_\varphi + \epsilon\,\bar{e}_y) \cdot \bar{e}_x = -\not{C} \sin\varphi\,,$$

$$V_y = \not{C}\,(\bar{e}_\varphi + \epsilon\,\bar{e}_y) \cdot \bar{e}_y = \not{C}\,(\cos\varphi + \epsilon).$$

Note that $V_z = 0$ since $\bar{V} \cdot \bar{e}_z$ vanishes, identically.

If equation (8) is squared, one obtains

$$V^2 \triangleq \bar{V} \cdot \bar{V} = \left(\frac{\mu}{h}\right)^2 (1 + 2\,\bar{e}_\varphi \cdot \bar{e}_y\,\epsilon + \epsilon^2) = \frac{\mu}{p}\,(1 + 2\,\epsilon \cos \varphi + \epsilon^2), \tag{10}$$

accounting for the fact that $p = h^2/\mu$. An inspection of this last expression leads to the conclusions that:

(a), for elliptic and hyperbolic motion $(1 + 2\,\epsilon \cos \varphi + \epsilon^2) > 0$; and,

(b), for parabolic motion $[2\,(1 + \cos \varphi)] \geq 0$.

Recalling that there is a limit position angle defined for motion on a hyperbolic path (i.e. as $r \to \infty$, $\varphi \to \varphi_{lim}$, where $\varphi_{lim} = \cos^{-1}(-1/\epsilon)$);

then the corresponding limit speed (squared) is,

$$V^2_{lim} \to \frac{\mu}{p}\,(\epsilon^2 - 1) \equiv \frac{\mu}{a}, \tag{11}$$

since $p = a(\epsilon^2 - 1)$ for the hyperbola. This last result is frequently referred to as the <u>hyperbolic excess speed</u> (squared); note that for a parabolic path $(\epsilon = 1)$,

$$V^2_{lim} \to 0.$$

Next, recalling that the eccentric anomaly $(\mathcal{E})$, for an elliptic path, can be related to the true anomaly by

$$\cos \varphi = \frac{\cos \mathcal{E} - \epsilon}{1 - \epsilon \cos \mathcal{E}}; \text{ or, } \cos \mathcal{E} = \frac{\epsilon + \cos \varphi}{1 + \epsilon \cos \varphi}; \tag{12}$$

then it can be shown that corresponding to equation (10)—making use of equation (7)—

$$V^2 = V_c^2\,(1 + \epsilon \cos \mathcal{E}), \tag{13}$$

wherein $V_c^2 \overset{\Delta}{=} \mu/r$ (local circular satellite speed (squared)). Here, equations (10) and (13) relate local speed to the local position angles (φ and $\mathcal{E}$). The geometric relation between φ and $\mathcal{E}$ will be described subsequently.

It should be mentioned here that equation (8) was derived primarily for the purpose of defining the hodograph; and, as noted above, it is not stated in a usual form. Figure 3 shows the various velocity elements, referred to previously, and some of the geometry relative to these vector elements.

Making use of the speed relations developed as equations (9) it is possible to establish many interesting analytic and geometric results. For instance; forming ratios of the various speed components leads to: (a) the trajectory eccentricity,

$$\epsilon \overset{\Delta}{=} \frac{|V_r|}{|V_x|}; \tag{14}$$

and, (b) the eccentric anomaly, corresponding to a point on the trajectory, described by,

$$\mathcal{E} = \cos^{-1}\left(\frac{V_y}{V_\varphi}\right). \tag{15}$$

Needless to say, it is possible to use these relations, in conjunction with the familiar definitions and descriptions of the orbital parameters, to derive useful and interesting analytic relations. However, this is not the purpose of this investigation; consequently, a different tact will be followed below.

A Description of the Hodograph

The velocity expression developed as equation (8) can be utilized, directly, to describe a hodograph for the two-body motions considered here. It will be seen that the development is amenable to either the (fixed) x,y,z - or (moving) r, φ, z - frames of reference noted in the introduction. Because of the similarity in manipulation for these two cases it is advantageous to conduct the developments in parallel and simultaneously:

The Special Hodograph (referred to the r, φ, z triad.) Write the velocity vector expression from equation (8) as:

$$\bar{V} = \not{C}(\bar{e}_\varphi + \epsilon\,\bar{e}_y) \equiv V_r\,\bar{e}_r + V_\varphi\,\bar{e}_\varphi\,, \qquad (16a)$$

The Classical Hodograph (referred to the x,y,z triad). Write the velocity vector equation as:

$$\bar{V} = \not{C}(\bar{e}_\varphi + \epsilon\,\bar{e}_y) \equiv V_x\,\bar{e}_x + V_y\,\bar{e}_y\,. \qquad (16b)$$

Next, rearrange this result into the following form(s):

$$(V_\varphi - \not{C})\,\bar{e}_\varphi + V_r\,\bar{e}_r = \epsilon\,\not{C}\,\bar{e}_y\,, \qquad (17a)$$

$$(V_y - \epsilon\,\not{C})\,\bar{e}_y + V_x\,\bar{e}_x = \not{C}\,\bar{e}_\varphi\,; \qquad (17b)$$

and, squaring the above expressions yields,

$$(V_\varphi - \not{C})^2 + V_r^2 = (\epsilon\,\not{C})^2 \qquad (18a)$$

$$(V_y - \epsilon\,\not{C})^2 + V_x^2 = \not{C}^2\,. \qquad (18b)$$

This expression describes a circle (on the V_φ, V_r plane). Its center is located at $\not{C}$ units along the V_φ axis; it has a radius of $\epsilon\,\not{C}(\stackrel{\Delta}{=}R)$.

This expression describes a circle of radius $\not{C}$ whose center is located at $\epsilon\not{C}$ units on the V_y axis.

A sketch of the special hodograph, and its relation to an elliptic orbit, is shown as Figure 4a, 4c.

A sketch relating the classical hodograph to a corresponding ellipse is noted on Figure 4b, 4c.

The geometries of Figure 4 have been chosen to represent the elliptic orbital motion; this selection was made with convenience of representation being the deciding factor. It should be evident, however, that the descriptions could have been made for the hyperbolic case just as well.

The cases illustrated on Figure 5 show a comparison of the hodographs, for several values of eccentricity, as these would appear on the two velocity planes (V_r, V_φ; V_x, V_y). It should be noted that the circular orbit, on the V_r, V_φ plane is the point, $\not{C}$; while in the V_x, V_y plane the hodograph is a circle of radius $\not{C}$ with its center at the origin of coordinates (i.e.; $\epsilon = 0$, hence $R = 0$). As the eccentricity increases the figure of the hodograph grows, in size, on the V_r, V_φ plane; while on the classical hodograph plane the center of the figure moves away from the coordinate origin. When the trajectory is a parabola the two hodographs appear to be markedly alike ($\not{C} \equiv R$; $\epsilon = 1$).

For the hyperbola, since $\epsilon > 1.0$, the hodograph (circle) on the V_r, V_φ plane has a radius (R) which is greater in value than the central position distance ($\not{C}$), hence the figure extends into the <u>negative</u> V_φ region; this last condition, of course, is unrealistic. When this case is referred to the V_x, V_y plane, the hodograph is a circle whose center lies above the origin. On this hodograph the inaccessible region is that which is shown cross-hatched on the figure. This region is bounded by the limit angle radii, where $\varphi_{lim} = \cos^{-1}(-1/\epsilon)$.

From the standpoint of geometry it should be apparent that the classical and special hodographs are most applicable, as motion representations, over different ranges of the eccentricity (ϵ).

A Geometric Description of the (Elliptic) Eccentric Anomaly, $\mathcal{E}$

Figure 6 shows, in schematic, the eccentric anomaly ($\mathcal{E}$) and the corresponding true anomaly (φ) for a representative position, P, on an elliptic trajectory. The point, P', lies on the (so-called) auxiliary circle (of radius, a) and corresponds to the trajectory point, P; the position coordinates for these two points are (a, $\mathcal{E}$) and (r, φ), respectively. In a subsequent section a geometric method for determining $\mathcal{E}$, from the hodograph, will be described using both of the hodograph planes mentioned earlier.

A Geometric Description of the (Hyperbolic) Anomalies (H, $\mathcal{E}_H$)

Figure 7 shows a construction to determine the angle H, which is a reference angle related to the hyperbolic true anomaly (φ). This angle (H) is described in the following manner:

Having drawn the hyperbola, and the auxiliary circle (radius = a); then for a point (P) on the hyperbola, locate Q directly below it. Through Q draw a tangent to the auxiliar circle; the point of tangency is denoted as P'. The radius vector locating P' has the coordinates (a,H) as seen on the figure.

It should be evident that the angular ranges of interest (here) for these two angles are;

$$0 \le |\varphi| \le \varphi_{lim},$$

where

$$\varphi_{lim} = \cos^{-1}\left(-\frac{1}{\epsilon}\right);$$

and

$$0 \leq |H| \leq \pi/2.$$

In support of the range given for H, one notes that $H \to 0$ as $\varphi \to 0$; and, that as P (hence r) moves to infinity, the line QP' tends to the horizontal with $H \to \pi/2$.

A development, linking H and $\mathcal{E}_H$, is found in reference 6, appendix 8B. From the results given there one finds that the conic equation can be expressed as

$$r = a\left(\frac{\epsilon}{\cos H} - 1\right). \tag{19}$$

When this is compared to the more usual expression, involving the hyperbolic analog to the eccentric anomaly; namely,

$$r = a\,(\epsilon \cosh \mathcal{E}_H - 1)$$

(See reference 5, pg 98), then it is apparent that

$$\cosh \mathcal{E}_H \equiv \sec H. \tag{20}$$

This expression shows the connecting relationship between these two quantities. In a similar manner the general conic expression

$$r = \frac{a(\epsilon^2 - 1)}{1 + \epsilon \cos \varphi},$$

can be equated to equations (19), (20) to give the following:

$$\cosh \mathcal{E}_H = \sec H = \frac{\epsilon + \cos \varphi}{1 + \epsilon \cos \varphi} \tag{21a}$$

$$\tanh \mathcal{E}_H = \sin H = \frac{\sqrt{\epsilon^2 - 1}\, \sin \varphi}{\epsilon + \cos \varphi}\,; \tag{21b}$$

and

$$\tan \frac{H}{2} = \sqrt{\frac{\epsilon - 1}{\epsilon + 1}}\, \tan \frac{\varphi}{2} = \tanh \frac{\mathcal{E}_H}{2}\,. \tag{21c}$$

These expressions have been obtained to properly align results and to facilitate an orderly description of the time equation, wherein $t \stackrel{\Delta}{=} t\,(\mathcal{E}_H)$. Also, the need for the angle H will become evident when a construction to obtain $\mathcal{E}_H$ is undertaken.

The Special Hodograph; Motion on an Ellipse

For the special hodograph the speed components (see equation (9)) are

$$V_r = e\,\cancel{C} \sin \varphi, \tag{22}$$

and

$$V_\varphi = \cancel{C}\,(1 + \epsilon \cos \varphi).$$

Let this hodograph be modified so that its coordinates are $V_r/\cancel{C}$ and $V_\varphi/\cancel{C}$. This does not alter the basic geometry even though the relative scale of the figure is changed. As a consequence of this transformation the hodograph is a circle having a radius equal to the trajectory's eccentricity; but, one having its center at a unit distance from the coordinate origin.

Since the eccentric and true anomalies are related by

$$\cos \mathcal{E} = \frac{\epsilon + \cos \varphi}{1 + \epsilon \cos \varphi}, \tag{23}$$

(see reference 5, page 85) then the following construction, based on this relation, determines the angle ($\mathcal{E}$). The several steps of the construction are found on Figure 8, and occur as listed below:

I. General Considerations

Draw a (modified) hodograph on the $V_r/\mathcal{C}$, $V_\varphi/\mathcal{C}$ plane; this is a circle of radius equal to the eccentricity, having its center at a unit distance along the $V_\varphi/\mathcal{C}$ axis. The center of the hodograph circle is noted by O.

The point (P) is a position of interest on the trajectory; it is located by φ (the true anomaly), and/or by $\mathcal{E}$, the eccentric anomaly (recall Figure 6).

II. Construction:

1. Using O as a center, draw a unit circle and extend OP to locate Q (on this unit circle). Note that OP = ϵ (units) while OQ = 1 (unit).

2. Project P onto the $V_r/\mathcal{C}$ axis locating point D; thus, the distance PD = OO' + OP $\cos \varphi$; or, PD = $1 + \epsilon \cos \varphi$.

3. Project Q onto the $V_\varphi/\mathcal{C}$ axis, locating Q_1; consequently O' $Q_1 = 1 + \cos \varphi$.

4. Extend the line QPO; then, using O as a center, transfer point Q_1 to QPO

(extended) locating point Q_2. Since $OQ_1 = \cos\varphi$, then $\underline{\underline{PQ_2}} = OP + OQ_2 \equiv \underline{\underline{\epsilon + \cos\varphi}}$.

5. At Q_2 erect a perpendicular (to POQ_2); and, using P as a center, transfer D to D_1 (D_1 is where the arc, of radius PD, cuts the perpendicular from Q_2). Since $PD = 1 + \epsilon\cos\varphi$, then $\underline{\underline{PD_1 = 1 + \epsilon\cos\varphi}}$.

6. According to equation (30) the angle at P, between PQ_2 and PD_1, is the eccentric anomaly for the point on the trajectory.

Basically, this completes the construction; however, before leaving this discussion note that the line through O, perpendicular to PD_1 and locating J, is the line

$$OJ = \epsilon \sin \mathcal{E},$$

since $OP = \epsilon$. The significance of this will be noted subsequently.

As a convenience, it is desirable to relocate the eccentric anomaly (relative to O); this is easily accomplished by erecting perpendiculars, through O, to the lines PQ_2 and PD_1. This last construction is illustrated on Figure 8b.

On this figure the arc $\mathcal{P}_1 Q$ corresponds to the position angle (φ) while the arc AA_1 corresponds to the eccentric anomaly ($\mathcal{E}$); both arcs are comparable since they relate to the unit circle.

The Classical Hodograph; Motion on an Ellipse

For this hodograph the speed components are

$$V_x = -\not{C} \sin\varphi$$

and

$$V_y = \not{C}(\epsilon + \cos\varphi), \tag{24}$$

(see equations (9)).

As in the previous construction it is best to work with a modified hodograph; thus, the coordinate axes are chosen as $V_x/\not{C}$ and $V_y/\not{C}$, respectively. Once again the construction will be based on equation (23); however, the steps to be followed are noted below and depicted on Figure 9a.

I. General Considerations

Construction on this plane is much simpler than that for the previous case. Here the hodograph is a unit circle with its center located at ϵ (units) along the $V_y/\not{C}$ axis.

II. Construction

With P being a point on the (elliptic) orbit located by the position angle. φ, then:

1. Project P onto the $V_y/\not{C}$ axis locating P_1. Note that OP $\equiv$ 1.0, thus $OP_1 = \cos\varphi$; also, $\underline{\underline{O'P_1}} = O'O + OP_1 = \underline{\underline{\epsilon + \cos\varphi}}$, since $O'O \equiv \epsilon$.

2. Erect a perpendicular to the line OP (extended) through O'; this will locate the point Q. With $OO' \equiv \epsilon$, then $OQ = \epsilon\cos\varphi$ and $\underline{\underline{PQ}} = PO + OQ = \underline{\underline{1 + \epsilon\cos\varphi}}$.

3. Using O' as a center, and PQ as a radius, swing an arc locating point D at the intersection of the arc and line PP_1.

Now, the eccentric anomaly ($\mathfrak{E}$) is noted to be the angle, at O', within the triangle whose base is $O'P_1$ and whose hypotenuse is O'D, as shown.

4. Note that the perpendicular erected through O, drawn normal to O'D (locating point J), describes a line whose length is

$$OJ = \epsilon \sin \mathcal{E}.$$

The significance of OJ will be indicated subsequently.

For purposes of comparison, the angle $\mathcal{E}$ is transferred to the origin (O) so that it may be directly related to the corresponding true anomaly (φ). Thus, on Figure 9b, the arc $\mathcal{P}$A describes $\mathcal{E}$, while the arc $\mathcal{P}$P defines φ; both of these angles refer to the point, P, on the ellipse. Similarly, the length OJ has been transferred to the horizontal on Figure 9b.

The Special Hodograph; Motion along a Hyperbolic Arc

As in the previous cases a modified hodograph is constructed with a general point P(r, φ) being selected for study. Figure 10a will illustrate the construction, which is described below; and, in addition it will note the relevant properties of this geometry.

I. General Conditions

On the plane ($V_\varphi/\mathcal{C}$, $V_r/\mathcal{C}$) draw a unit circle which is tangent to the origin. The modified hodograph is the circle, centered at O, having a radius of ϵ (units). The radii to points where this circle cuts the $V_r/\mathcal{C}$ axis bound the region of the hodograph which is inaccessible to this motion; incidentally, this zone corresponds to arcs on the second branch of the hyperbolae.

Locating P on the hodograph, at φ relative to the $\frac{V_\varphi}{\not{C}}$ axis, then the construction to determine H, according to equation (21a), is outlined below. Note that

$$\cos H = \frac{1 + \epsilon \cos \varphi}{\epsilon + \cos \varphi} \; . \tag{25}$$

II. Construction

1. The radius OQ cuts the unit circle at P. Projecting P and Q onto the $\frac{V_\varphi}{\not{C}}$ axis locates Q_1 and P_1, with $OQ_1 = \epsilon \cos \varphi$, and $OP_1 = \cos \varphi$.

2. Projecting Q onto the $\frac{V_r}{\not{C}}$ axis located D; thus, $\underline{\underline{QD}} \equiv O'O + OQ_1 = \underline{\underline{1 + \cos \varphi}}$.

3. Extend line PO; and, using OP_1 as a radius, transfer P_1 to P_2 (on PO extended). Since $OP_2 \equiv OP_1$ then $P_2Q = \epsilon + \cos \varphi$.

4. Using Q as a center, swing an arc (radius P_2Q), transferring P_2 to P_3. Point P_3 is at the intersection of this arc and the $\frac{V_r}{\not{C}}$ axis; note that $\underline{\underline{P_3Q}} \equiv \underline{\underline{\epsilon + \cos \varphi}}$.

It is evident, now, that the angle H, at Q, is formed by the lines QD and P_3Q, according to the relations given by equation (25).

To transfer the angle H, from Q to O as a central position, erect perpendiculars (through O) to lines QD and P_3Q. Then, the arc AA_1 will correspond to H while the arc $\mathcal{P}P$ corresponds to φ.

Unfortunately H is not the angle describing the analog to the eccentric anomaly. To find $\mathcal{E}_H$, the analogous anomaly, it is necessary to do the computation indicated by equations (20). One advantage here, however, is that one knows (a priori) the extent of H for the admissible range of φ. That is, H will vary from 0 to $\pi/2$ while φ varies from 0 to $\cos^{-1}(-1/\epsilon)$.

The Classical Hodograph; Motion along a Hyperbolic Arc

The construction for this case is analogous to that carried out above, but differing according to the conceptual geometry associated with this representation. The basic difference stems from the fact that the hodograph circle (of unit radius) is centered at ϵ (units) above the origin, O' (see Figure 10b). The inaccessible arc on this mapping is between the radii positioned at $\pm \varphi_{lim}$; this positioning is described by the lines tangent to the hodograph drawn through the origin O'. In order to determine the angle (H), corresponding to a general point (P), one can develop a construction based on the use of equation (25), as before. Such a procedure follows below:

I. General Considerations

The modified hodograph is drawn on the $\left(\frac{V_x}{\cancel{C}}, \frac{V_y}{\cancel{C}}\right)$ plane as a unit circle with center (O) located at ϵ on the $V_y/\cancel{C}$ axis. Using O as a center draw a concentric circle of radius ϵ. Locate the test point (P) on the hodograph at its proper position, φ .

II. Construction

1. Project point P on the $\frac{V_y}{\cancel{C}}$ axis, locating point P_1 . Note that $OP_1 = \cos\varphi$, since $OP = 1.0$.

2. Extend the line PO, downward, and erect a perpendicular to this extension through O'. With $O'O = \epsilon$, then $OQ = \epsilon \cos\varphi$ and $\underline{PQ = 1 + \epsilon \cos\varphi}$.

3. Transfer the line PQ parallel to itself until the line $O'P'$ ($\equiv QP$) is described.

4. Since $O'O = \epsilon$ and $OP_1 = \cos\varphi$ then line $O'P_1 = \epsilon + \cos\varphi$. Using this as a radius, and O' as a center, find the intersection of this arc with the line from P to P'. This intersection is denoted as P_2; thus $\underline{\underline{O'P_2 = \epsilon + \cos\varphi}}$ and the angle H is determined.

According to the description above, H is the angle at O' between the lines $O'P_2$ and $O'P'$, for the triangle $O'P'P_2$.

To transfer H to the center, O, draw perpendiculars to O'P' and $O'P_2$ passing through O. As before the arc AA_1 corresponds to the angle H, while arc $\mathcal{P}P$ corresponds to φ.

The Time Equation

It can be shown (see reference 5, pg. 86) that the time of flight, from pericenter along an elliptic path, expressed in terms of the eccentric anomaly, is

$$n(t - \tau) = \mathfrak{E} - \epsilon \sin \mathfrak{E}, \tag{26}$$

where n is the mean motion and τ is the time of pericenter passage.

Referring to the construction for the eccentric anomaly, it is evident that all information needed to evaluate this time expression has been determined. The arc defining $\mathfrak{E}$, and the line OJ ($= \epsilon \sin \mathfrak{E}$), have been constructed; hence, by subtracting the two numbers - one describing the arc for $\mathfrak{E}$, the other being OJ - the time function, $n(t - \tau)$ is determined.

As an alternate description, the length OJ can be converted to an equivalent angle (since the basic hodograph geometry has been referred to a unit circle) so that the difference between $\mathcal{E}$ and this equivalent angle represents $n(t - \tau)$. It is usual to refer to this angle difference as the Mean Anomaly, M.

In connection with these statements a modified hodograph diagram, showing relative sizes of the angles (M, $\mathcal{E}$, φ), is presented as Figure 11a. On the figure are several (corresponding) angular combinations; these are provided to indicate the relative extent of the various angles and the corresponding relative variations of these as points are followed about the elliptic orbit. These sets of angles are denoted as φ_i, $\mathcal{E}_i$, M_i (i being the indicator for points P_i along the trajectory).

To solve the time equation for motion along a hyperbolic path, with time measured from pericenter, the analog to Kepler's equation (see reference 5, page 98),

$$n_H(t - \tau) = \epsilon \sinh \mathcal{E}_H - \mathcal{E}_H, \tag{27}$$

could be employed. Herein n_H is analogous to the elliptic mean motion, and τ is the time of pericenter passage; for reference, $n_H = \sqrt{\frac{\mu}{a^3}}$, where a is the semimajor axis length for the hyperbolic path (also, see equation (11)).

An analog to the mean motion (M), as would be applied to hyperbolic paths, can be expressed by

$$M_H = n_H (t - \tau) \tag{28}$$

Finally, as an aid to correlating the results from this section, a plot showing typical set of values of φ, H, $\mathcal{E}_H$, M_H, for an assumed ϵ (> 1.0) has been prepared. These data are presented on Figure 11b; however, it should be recalled that only φ and H are available from the construction; the values $\mathcal{E}_H$, M_H are obtained from appropriate arithmetic operations.

CONCLUSIONS

The developments carried out in this paper were aimed at illustrating the utility of the hodograph as a tool for obtaining useful information regarding certain aspects of a two-body central field motion. If the usual hodographic representation is altered, so that a modified form of the hodograph is described, then a graphical means for determining the eccentric anomaly, and its hyperbolic analog, is obtained. Also, from this construction one is able to obtain information, geometrically, which either directly, or indirectly, describes the time of motion (from pericenter) to a point on the trajectory.

These are but a few examples which illustrate the utility of the hodograph; not simply as a geometric adjunct to analytic results, but as a means for the development and simplification of analytic relations. Once this technique has been mastered it should prove to be a useful added device to the more usual tools employed in trajectory design and analysis.

REFERENCES

1. Altman, S. P., Orbital Hodograph Analysis, Vol. 3, AAS Science and Technology Series, Western Periodicals, 1965.

2. Altman, S. P. and Pistiner, J. S., "Hodograph Analysis of the Orbital Transfer Problem for Coplanar Nonaligned Elliptical Orbits", ARS Journal Vol. 31, September 1961.

3. Sun, F. T., "On the Hodograph Method for Solution of Orbital Problems:, Proceedings of the 12th International Astronautical Congress, Academic Press, New York, 1963.

4. Eades, J. B., The Hodograph and Its Application to Space Flight, Bulletin No. 157, Virginia Engineering Experiment Station, VPI, Blacksburg, Virginia, December 1964.

5. Roy, A. E., The Foundations of Astrodynamics, The Macmillan Co., New York, 1965.

6. Seifert, H. (Ed.), Space Technology, John Wiley and Sons, New York, 1959.

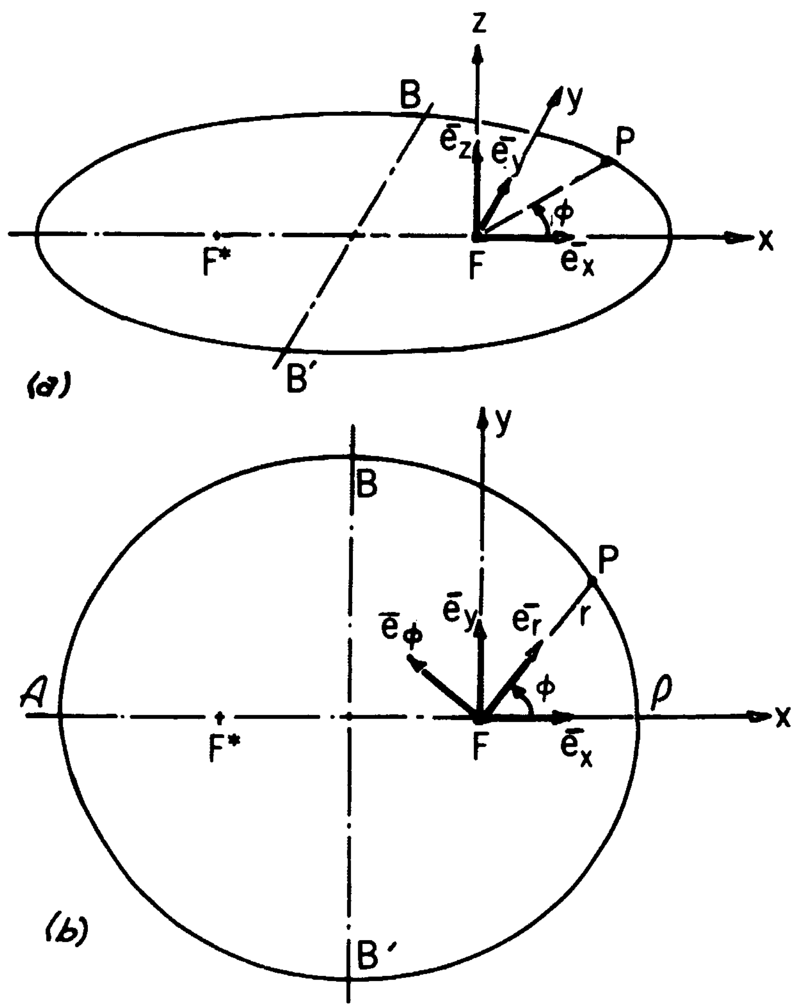

Figure 1—Basic geometry for a two-body (elliptic) trajectory, showing the two representative frames of reference. In sketch (a) the $\bar{e}_z$ vector is normal to the orbital plane. Sketch (b) shows the plane of motion; P is a general point on the ellipse; F and F* are the occupied and unoccupied foci, respectively; the line BB′ is the minor axis.

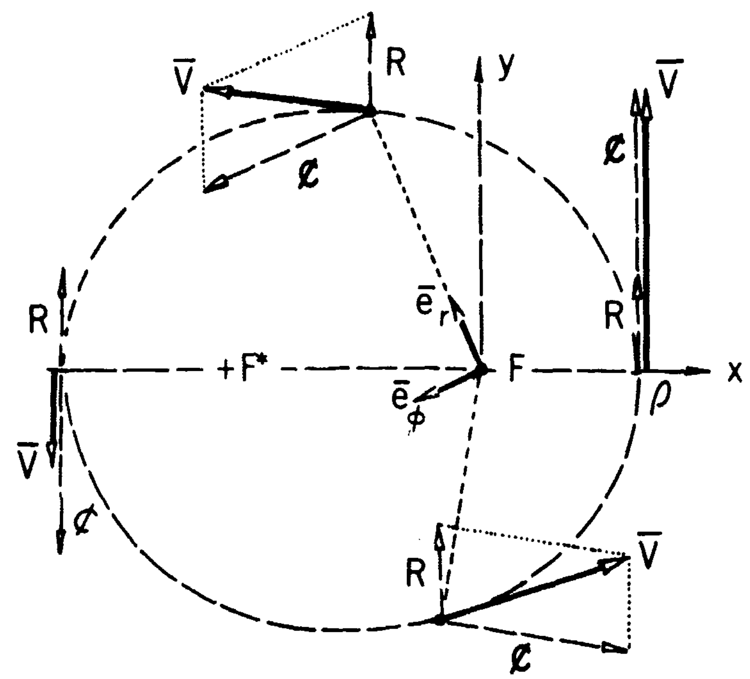

Figure 2–A sketch of the velocity vector, for central field conical motion, where

$$\bar{V} = \frac{\mu}{h}(\bar{e}_\varphi + \epsilon\,\bar{e}_y) = \bar{V}(\varphi) + \bar{V}(y)$$

with

$$\bar{V}(\varphi) = \frac{\mu}{h}\,\bar{e}_\varphi \stackrel{\Delta}{=} \mathcal{C}\,\bar{e}_\varphi$$

and

$$\bar{V}(y) = \epsilon\frac{\mu}{h}\,\bar{e}_y \stackrel{\Delta}{=} R\,\bar{e}_y$$

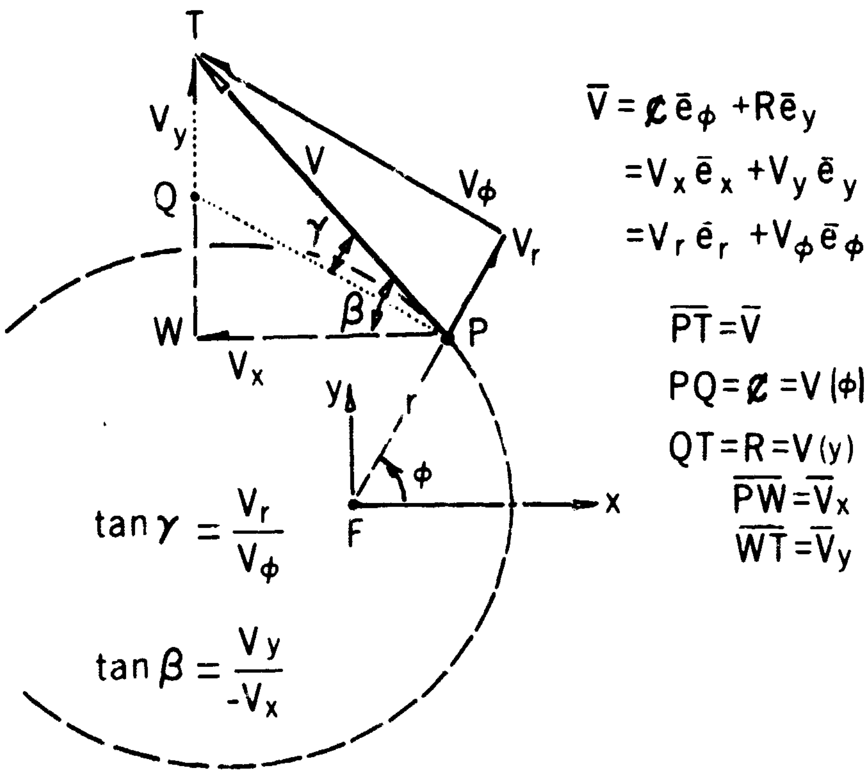

Figure 3–Velocity Components and Velocity Elements. Also, the elevation angles(γ, β), used to locate the velocity vector relative to the triads ($\bar{e}_r$, $\bar{e}_\varphi$, $\bar{e}_z$) and $\bar{e}_x$, $\bar{e}_y$, $\bar{e}_z$), are described.

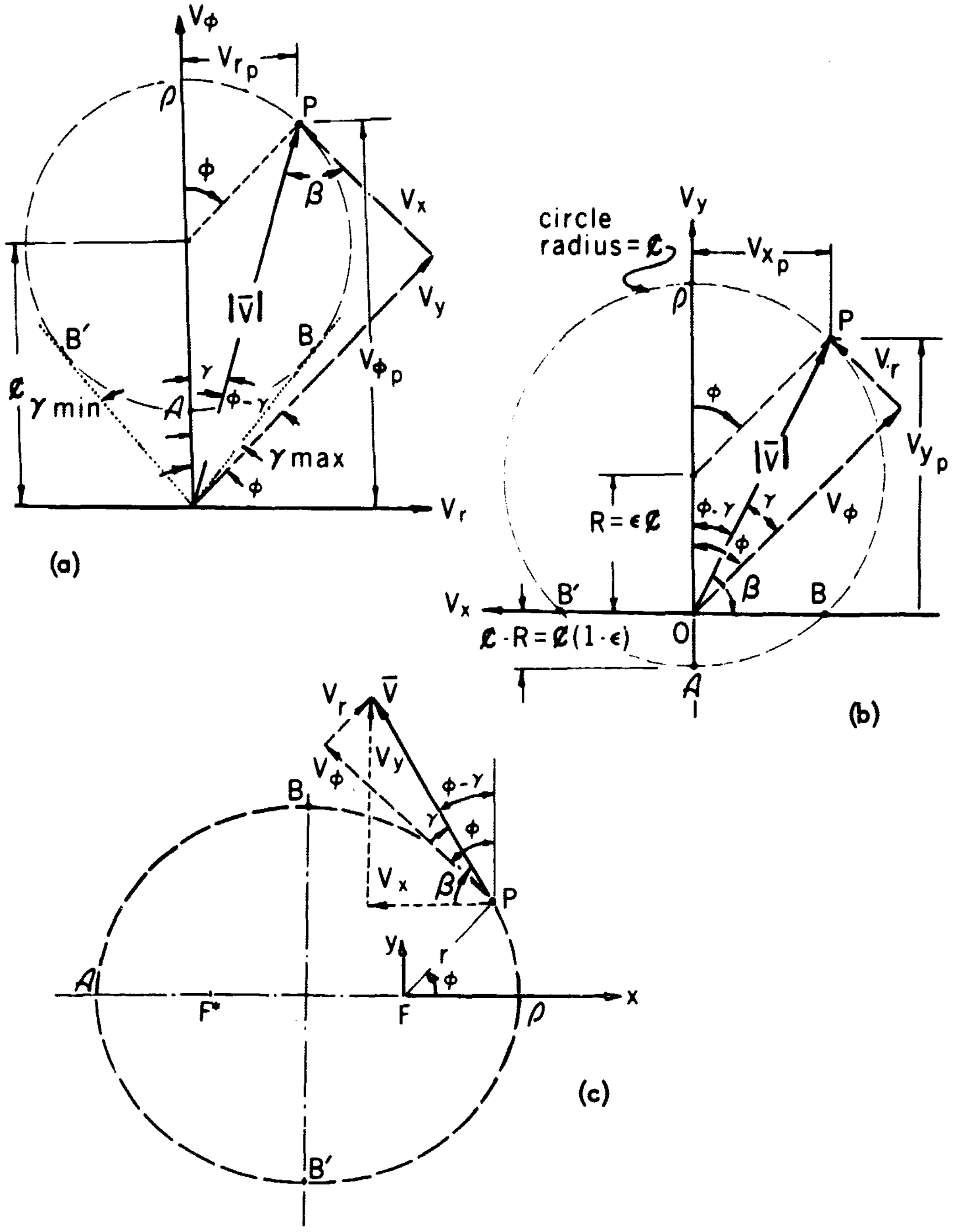

Figure 4–Sketch of the hodograph(s), corresponding to an ellipse of motion, on the Special Hodograph plane and on the Classical Hodograph plane. The positions ($\mathcal{P}$, $\mathcal{A}$) represent pericenter and apocenter, respectively. On both hodographs the velocity components and reference angles are noted.

(a) The Special Hodograph
(b) The Classical Hodograph
(c) The Ellipse of motion (F, F* are the occupied, unoccupied foci; P is a general point).

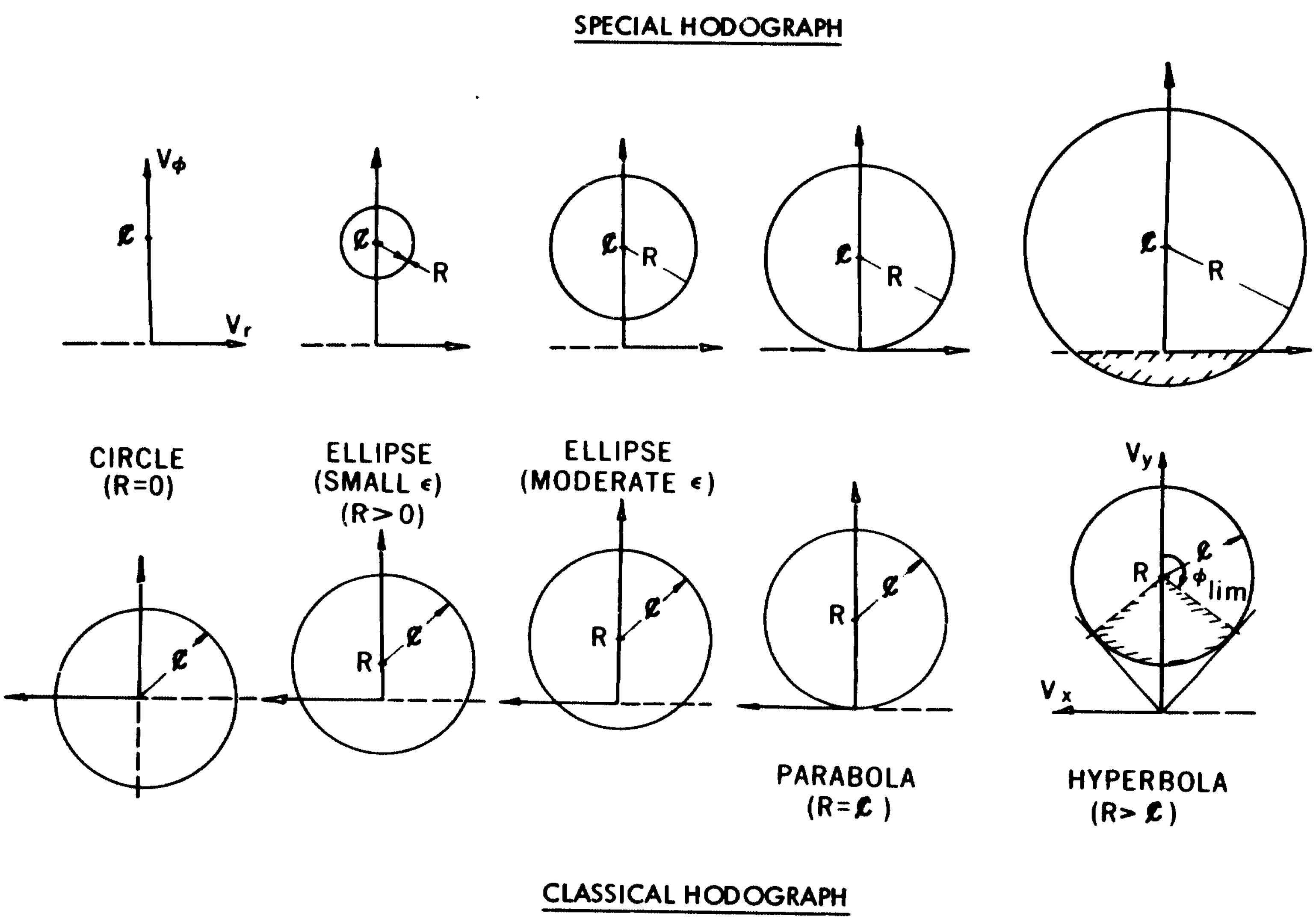

Figure 5–Sketch showing the relative geometries of the hodographs, for a given motion, on the V_r, V_φ, and V_x, V_y planes. For comparison, a constant value of $\mathfrak{C}$ has been assumed.

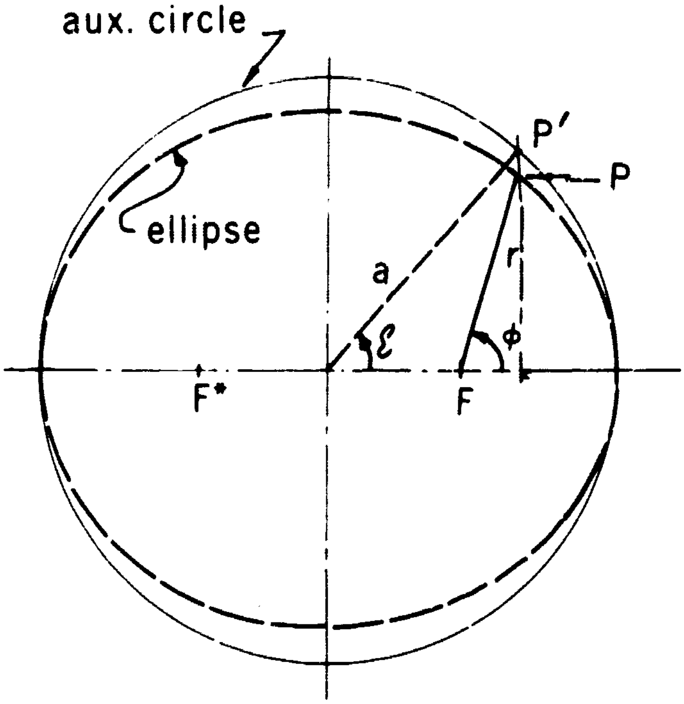

Figure 6–Sketch showing an elliptic trajectory, the corresponding auxiliary circle, and the anomalies (φ and $\mathcal{E}$) of a point P.

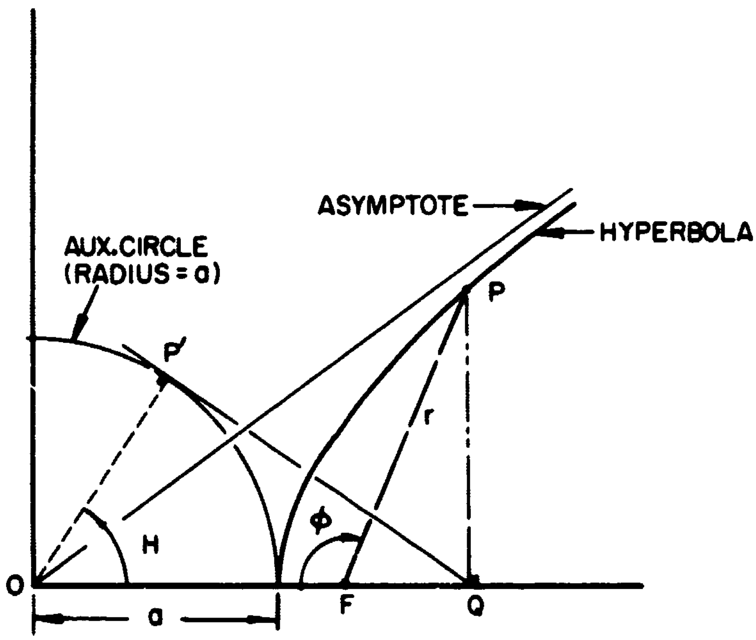

Figure 7–Sketch of the hyperbolic trajectory, the auxiliary circle and the position angles (φ and H) locating a point P.

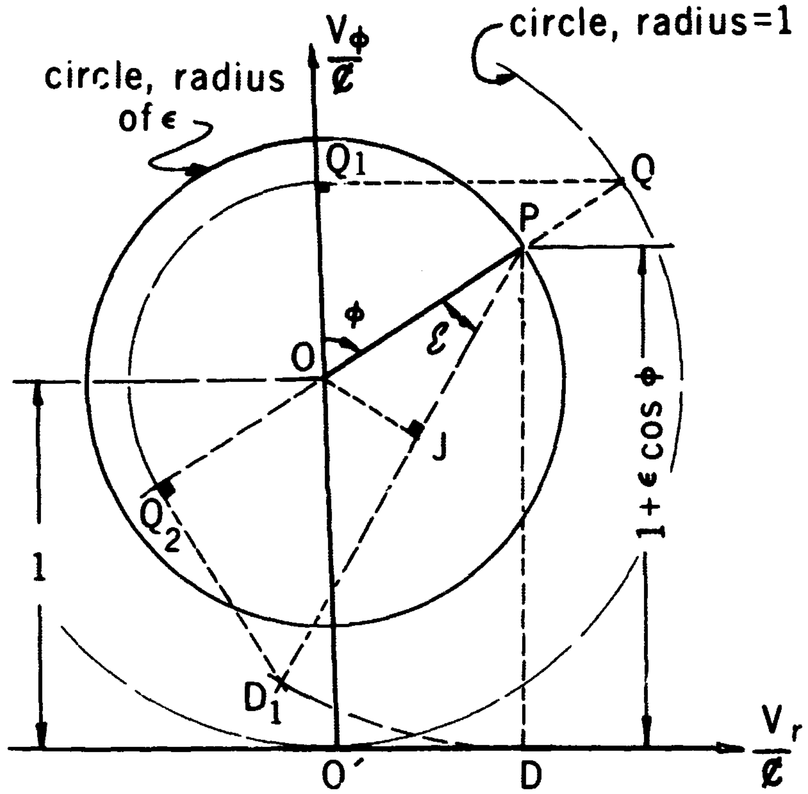

Figure 8a–The modified hodograph and a graphical description of eccentric anomaly, $\mathcal{E}$.

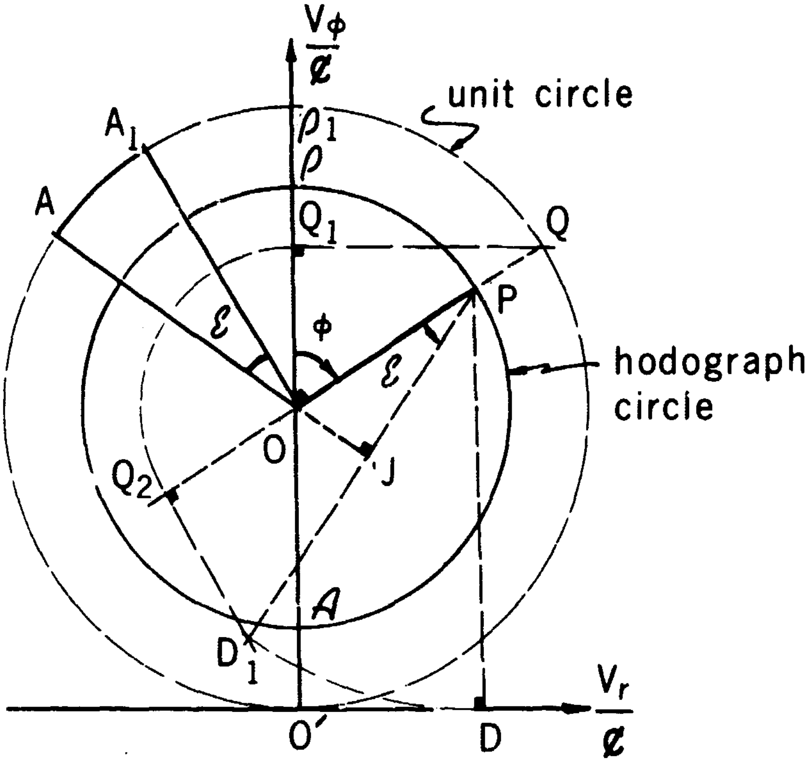

Figure 8b—Relocation of the eccentric anomaly, relative to the circular origin, O. The arc AA_1 defines $\mathcal{E}(P)$, while the arc from $\mathcal{P}_1$ to Q describes $\varphi(P)$.

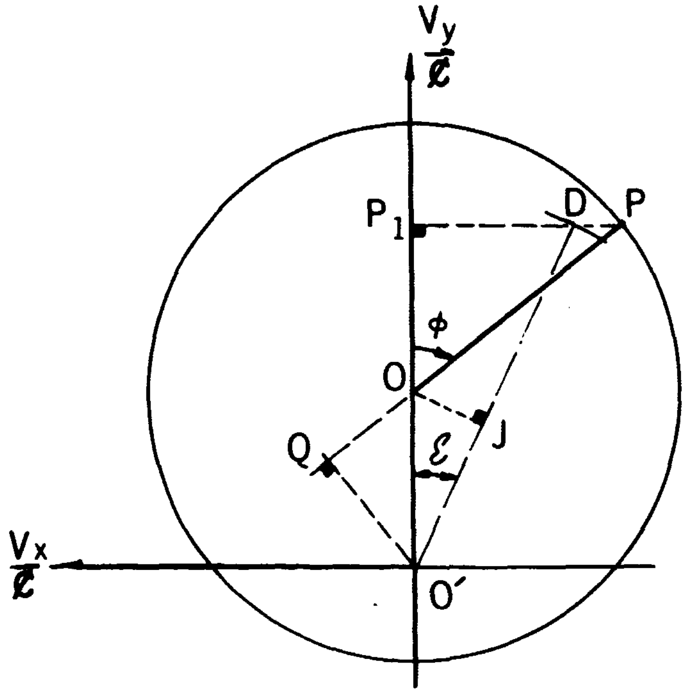

Figure 9a–A construction for the eccentric anomaly, ℰ, on the Classical Hodograph plane (modified).

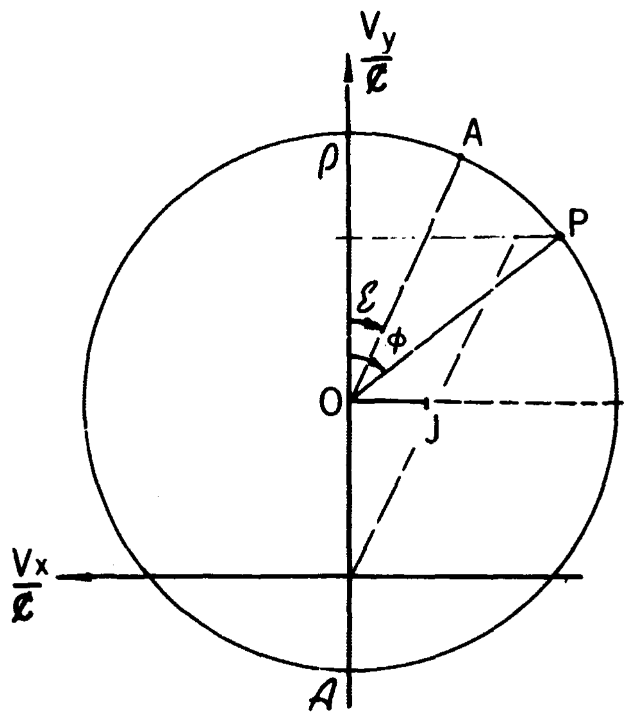

Figure 9b–The Relocation of ℰ(P) relative to the hodograph origin, O.

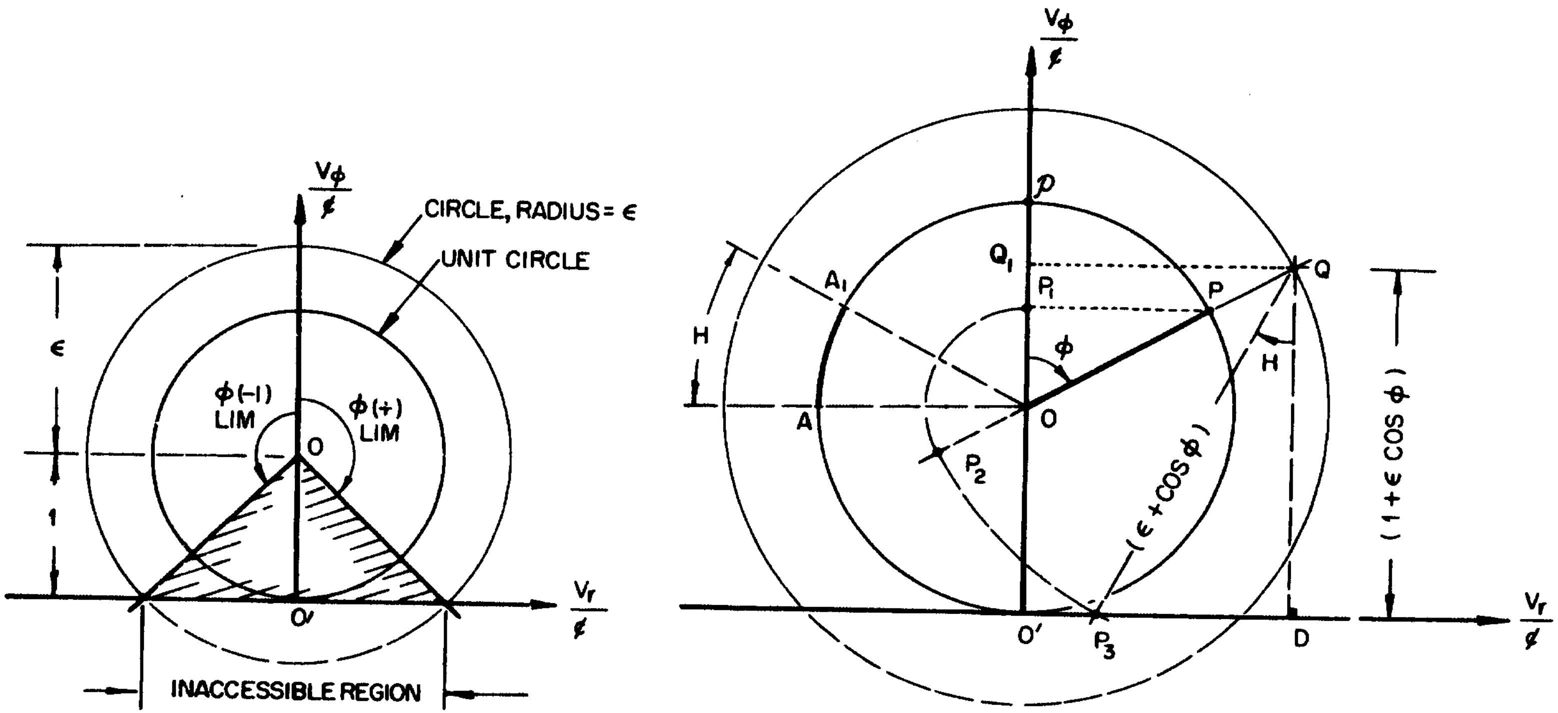

Figure 10a–A graphical description of H, constructed on the modified Special Hodograph plane.

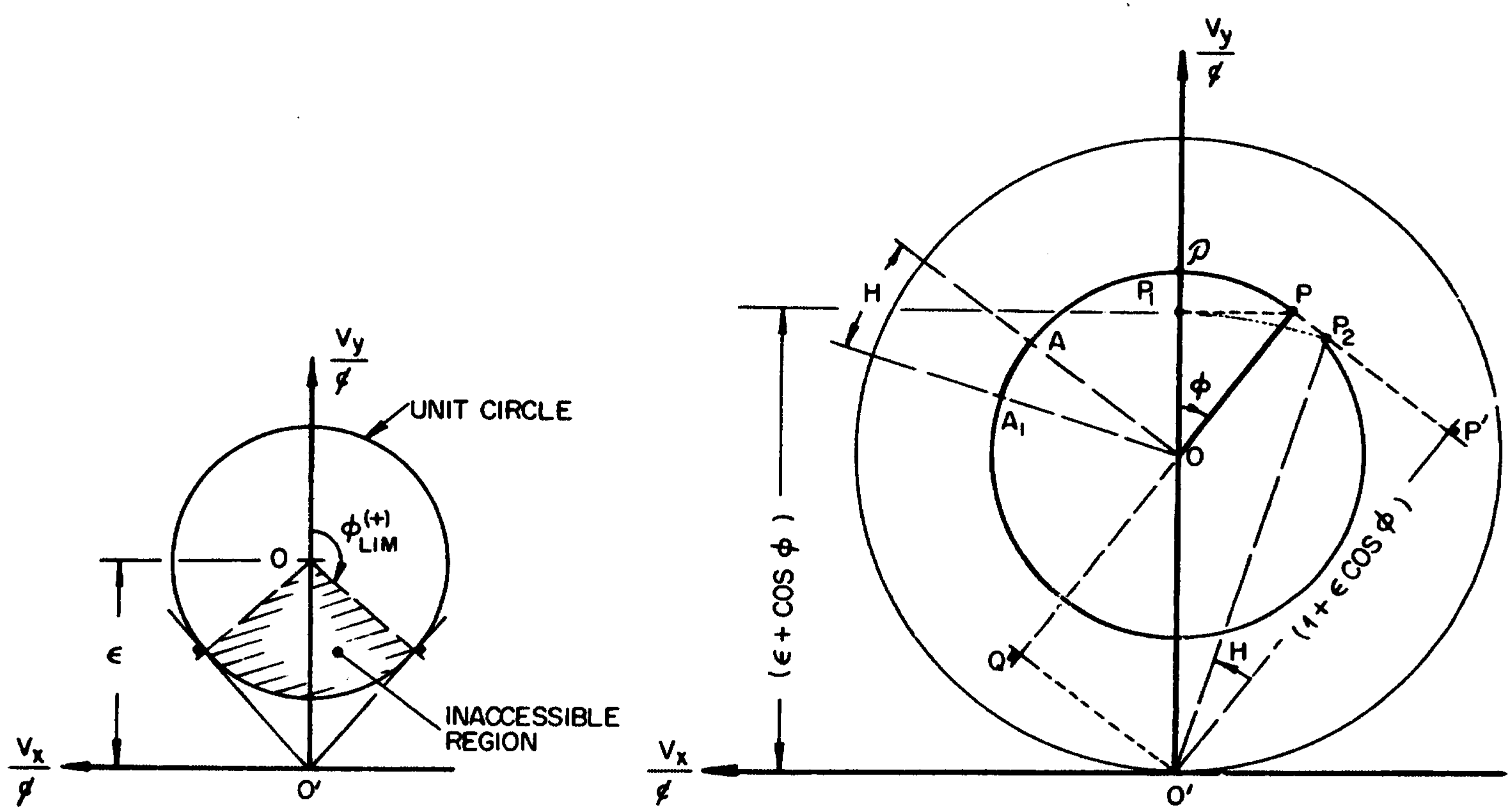

Figure 10b–A graphical description of the hyperbolic position angle H, on the modified Classical Hodograph plane. Note: H is also relocated relative to the origin O.

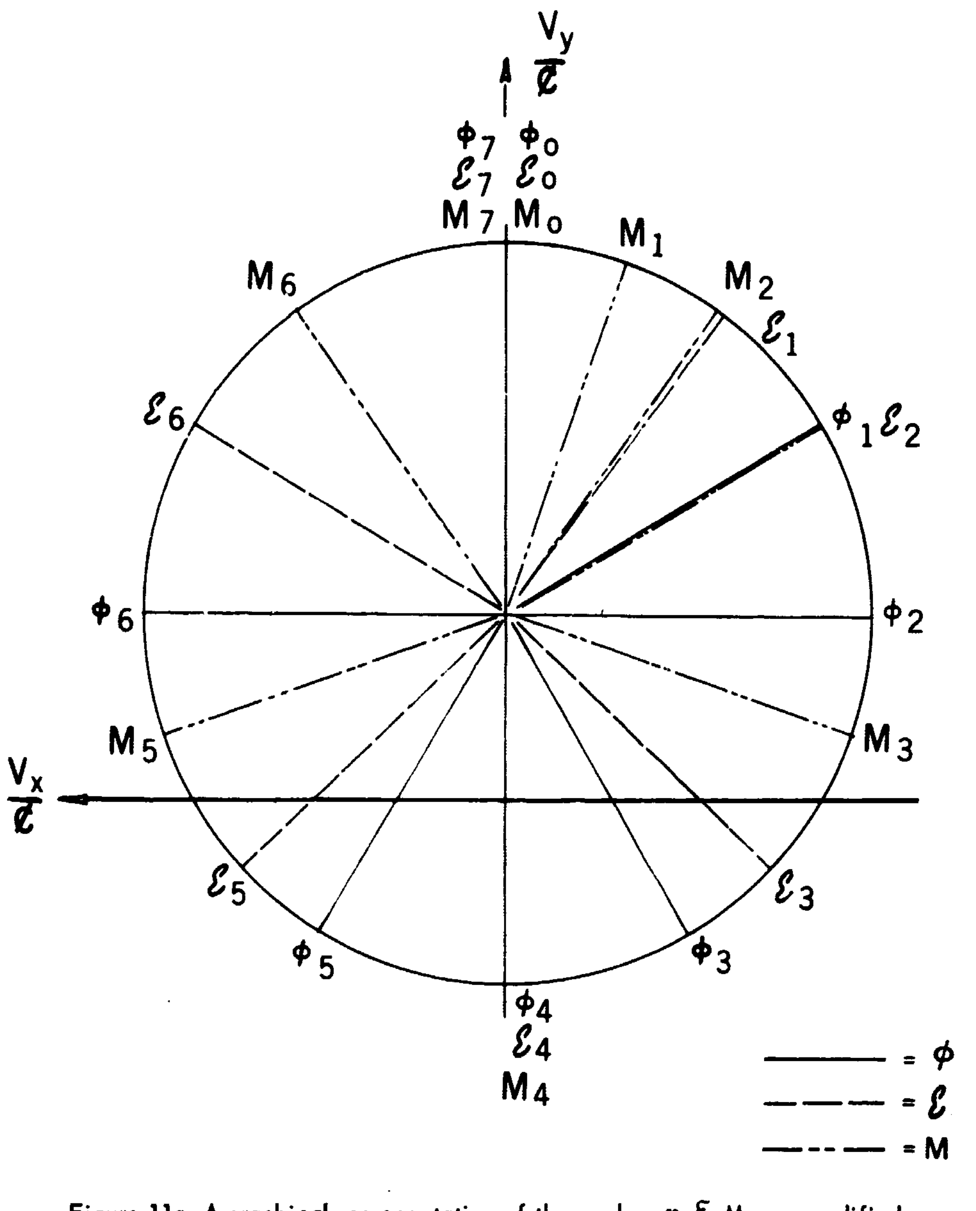

Figure 11a–A graphical representation of the angles φ, $\mathcal{E}$, M on a modified Classical Hodograph plane. The indices are used to correlate the various angle sets.

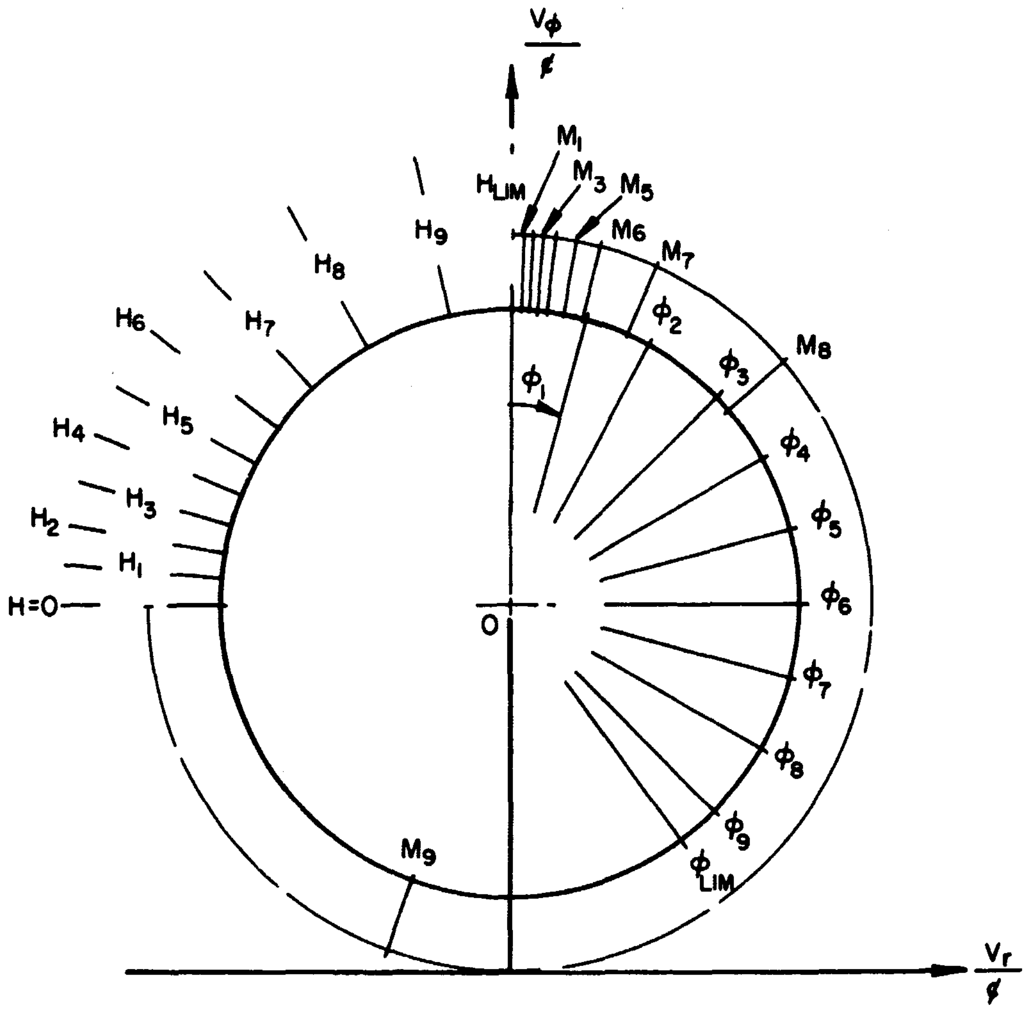

Figure 11b–A correlation for φ, H, M_H on the modified Special Hodograph for a typical hyperbolic trajectory. Indices are used to identify corresponding angles.